

## Theory of the Band Structure of Very Degenerate Semiconductors

P. A. WOLFF

*Bell Telephone Laboratories, Murray Hill, New Jersey*

(Received November 10, 1961)

In very degenerate semiconductors it is possible to achieve a situation in which the parameter  $r_s$  that characterizes the strength of electron-electron or electron-impurity interactions is small compared to unity. In this limit, many-body perturbation theory may be used to study certain properties of the system. We here consider the density of states for such a semiconductor, writing this quantity in terms of the electron propagator and self-energy. It is shown that the effect of electron-electron interactions is to screen impurity fields, and produce a nearly rigid downward motion of the energy band. For electrons near the Fermi surface the influence of impurity potentials is small; in particular, the diagonal matrix element of the impurity potential is exactly canceled by the corresponding electron-electron interaction term. As one proceeds lower into the band the electron-impurity interaction becomes progressively more important, and the straightforward perturbation theory appears to diverge for energies less than  $r_s^{\frac{1}{2}}$  times the Fermi energy. A propagator modification technique is suggested for extending the range of perturbation theory.

### I.

THE discovery of the Esaki diode has, in the past few years, stimulated considerable interest in the properties—particularly the band structure—of very degenerate semiconductors. A number of theoretical papers<sup>1</sup> have addressed themselves to this problem but, to date, no treatment has been given that proceeds from first principles, taking proper account of both electron-electron and electron-impurity interactions. This is not, perhaps, surprising since in its full generality the problem is an exceedingly complex one. There is, however, a certain limit—namely that of high density—in which, because of the exclusion principle, electrons acquire large kinetic energies and interaction effects become relatively small. Here a form of perturbation theory may be used to evaluate the properties of the system. The first successful application of this viewpoint is the calculation, by Gell-Mann and Brueckner,<sup>2</sup> of the correlation energy of the dense electron gas. Since then it has become clear<sup>3</sup> that the high-density limit is not reached in metals. Rather surprisingly, however, it *can* be attained in heavily-doped semiconductors. The crucial parameter that delineates the high-density regime is the quantity  $r_s$ , defined as the ratio of inter-electron spacing to Bohr radius. When this number is small compared to unity the system is in the high-density range. For good metals the interparticle spacing is one or two angstroms and  $r_s$  is typically 2–5. In a heavily-doped semiconductor, on the other hand, the interparticle spacing is much larger ( $10^{-6}$ – $10^{-7}$  cm) but the Bohr radius is also, in general, increased by a change in effective mass and dielectric constant. The latter effect often outweighs the former. For example, in InSb, where  $m^*/m \approx 0.01$  and  $\epsilon \approx 10$ , the Bohr radius is increased by a factor 1000 and one finds, for an electron density of  $10^{18}/\text{cc}$ , that  $r_s$  is about 1/5. This is a rather extreme case, but similar calculations for other

semiconductors indicate that the degenerate materials commonly used in Esaki diodes often lie in the dense ( $r_s \lesssim 1$ ) range. Thus, the methods of Gell-Mann and Brueckner should be useful for investigating their properties. One cannot expect, since  $r_s$  is never really small compared to unity, to attain high precision with such an approach, but the calculations should give a semiquantitative picture of the band structure and have, in addition, the great advantage of proceeding directly from first principles.

We shall focus our attention on the density of states of the degenerate semiconductor, though other properties can also be calculated with the methods we describe. Starting from an exact expression for this quantity, we shall evaluate it with the diagrammatic techniques—in particular, those discussed by Luttinger and Ward<sup>4</sup>—that seem to provide the most natural expression of perturbation theory. Within this framework, the treatment of electron-electron correlations is (to lowest order in  $r_s$ ) quite straightforward. Their principal role is to screen, in essentially the Debye-Hückel manner, the various Coulomb potentials in the problem. In addition, they give rise to a nearly rigid, downward motion of the conduction band.

Our problem is further complicated, as compared to that of the free electron gas, by electron-impurity interactions. For electrons that lie near the Fermi surface these also may be treated with perturbation theory and, actually, have a rather minor effect on the band structure. Further down in the band, however, they are much more important; indeed, the straightforward perturbation theory appears to diverge for electrons whose energies are less than about  $r_s^{\frac{1}{2}}$  times the Fermi energy. Propagator modification techniques, of the type developed by Brueckner<sup>5</sup> and first applied to impurity band problems by Klauder,<sup>6</sup> can be used to extend the convergence of the theory. No detailed calculations using these techniques are presented in this

<sup>1</sup> P. Aigrain and J. des Cloiseaux, *Compt. rend.* **241**, 849 (1955); R. H. Parmenter, *Phys. Rev.* **97**, 587 (1955).

<sup>2</sup> M. Gell-Mann and K. A. Brueckner, *Phys. Rev.* **106**, 364 (1957).

<sup>3</sup> D. F. Dubois, *Ann. Phys.* **7**, 174 (1959); **8**, 24 (1959).

<sup>4</sup> J. M. Luttinger and J. C. Ward, *Phys. Rev.* **118**, 1417 (1960).

<sup>5</sup> K. A. Brueckner, in *The Many-Body Problem* (John Wiley & Sons, Inc., New York, 1959).

<sup>6</sup> J. R. Klauder, *Ann. Phys.* (to be published).

paper, but a number of the basic formulas are presented and discussed. Their evaluation, which we hope to present in a later publication, should provide further insight into the range of validity of the perturbation method.

## II.

Throughout the rest of this paper we will be concerned with a many-electron system described by the Hamiltonian

$$H = \sum_i \left( \frac{\mathbf{p}_i^2}{2m} \right) + \frac{1}{2} \sum_{i \neq j} \left( \frac{e^2}{\epsilon |\mathbf{r}_i - \mathbf{r}_j|} \right) - \sum_{i,I} \left( \frac{e^2}{\epsilon |\mathbf{r}_i - \mathbf{R}_I|} \right), \quad (1)$$

in which the  $\mathbf{r}_i$ 's are electron coordinates, the  $\mathbf{R}_I$ 's positions of randomly distributed impurities,  $\epsilon$  is the dielectric constant, and  $m$  the effective mass. This expression for  $H$  presupposes the effective-mass approximation (which should be valid here since we will be considering energies small compared to band gaps in common semiconductors), and also assumes a spherical band structure. A more basic assumption is that the kinetic energy term in Eq. (1) is the dominant one. We will generally assume this to be the case and treat the last two terms, which we collectively label  $V$ , as perturbations.

Our first task in studying this Hamiltonian is to develop an expression for the density of states. Here it is well to recall the sort of experiment one might use to measure this quantity. A typical example is a recombination experiment in which one measures the spectrum of radiation emitted by electrons as they drop from the conduction band to some lower lying, sharp level of the crystal. A complete description of this process is quite complicated. However, if we assume a constant optical matrix element and that the electron in the sharp level is uncorrelated with those in the conduction band, then the spectrum gives a direct measure of what might be called the one-particle density of states in the conduction band. It is the number of ways of removing a single electron from the conduction band with the resultant  $(N-1)$  electron system ending up in a state of definite energy. Such a definition does not count all possible excited states of the many-body system. It is, however, close to what is measured experimentally, and reduces to the usual result if one neglects electron-electron interactions.

With these remarks in mind, we define the density of states (we set  $\hbar=1$ ) at energy  $\omega$  by

$$\rho(\omega) = \sum_{\alpha, \mathbf{p}} \{ |(\psi_{\alpha}^{N-1}, a_{\mathbf{p}} \psi_0^N)|^2 \delta(E_{\alpha}^{N-1} + \omega - E_0^N) \}, \quad (2)$$

where  $\psi_0^N$  is the ground state (including interactions) of the  $N$ -electron system described by the Hamiltonian  $H$ , the  $\psi_{\alpha}^{N-1}$ 's are various states of the  $(N-1)$ -body system that remains after the electron in momentum state  $\mathbf{p}$  is destroyed by the annihilation operator  $a_{\mathbf{p}}$ , and  $E_0^N$  and  $E_{\alpha}^{N-1}$  are the corresponding energies. This ex-

pression for  $\rho$  is written in the momentum representation. One may easily show, however, that the formula is independent of basis and that the subscript  $\mathbf{p}$  could be used to index any complete set of annihilation operators. A more convenient form of Eq. (2) is obtained by making use of a representation of the delta functions which gives

$$\rho(\omega) = \frac{1}{2\pi i} \sum_{\alpha, \mathbf{p}} \left\{ |(\psi_{\alpha}^{N-1}, a_{\mathbf{p}} \psi_0^N)|^2 \times \left[ \frac{1}{(E_{\alpha}^{N-1} + \omega - E_0^N - i\eta)} - \frac{1}{(E_{\alpha}^{N-1} + \omega - E_0^N + i\eta)} \right] \right\}, \quad (3)$$

where, as usual,  $\eta$  is a small positive number.

Ultimately we wish to use diagrammatic techniques to evaluate Eq. (3). Their use, in problems involving impurity interactions, has been discussed by Langer.<sup>7</sup> Comparison with his work shows that  $\rho(\omega)$  is directly related to the single particle propagator. A simple calculation gives the result

$$\rho(\omega) = \frac{1}{2\pi} \text{Im} \sum_{\mathbf{p}} [\theta(\mu - \omega) S(\mathbf{p}, \mathbf{p}; \omega)], \quad (4)$$

where  $\theta$  is a step function,  $\mu$  the chemical potential and  $S(\mathbf{p}, \mathbf{p}; \omega)$  the diagonal element of the propagator (which here depends on two momentum variables since momentum is not conserved in electron-impurity scatterings). The step function appears in this expression because the only filled states are those which lie below the Fermi level.

Equation (4) gives the density of states for a particular distribution of the impurities. Kohn and Luttinger<sup>8</sup> have shown, however, that for random impurity distributions expressions of this kind can be replaced by their average over impurity configurations. Replacing Eq. (4) by its average gives

$$\rho(\omega) = \frac{1}{2\pi} \text{Im} \sum_{\mathbf{p}} [\theta(\mu - \omega) \bar{S}(\mathbf{p}, \omega)], \quad (5)$$

where  $\bar{S}(\mathbf{p}, \omega)$  is the averaged propagator defined by Langer. The physical meaning of this result is made clearer by writing  $\bar{S}(\mathbf{p}, \omega)$  in terms of the self-energy  $\Sigma(\mathbf{p}, \omega)$ . Following Langer we have

$$\bar{S}(\mathbf{p}, \omega) = \left[ \frac{1}{\omega - \mathbf{p}^2/2m - \Sigma(\mathbf{p}, \omega)} \right]. \quad (6)$$

<sup>7</sup> J. S. Langer, Phys. Rev. **120**, 714 (1961).

<sup>8</sup> W. Kohn and J. M. Luttinger, Phys. Rev. **108**, 590 (1957).

Writing  $\Sigma$  in terms of its real and imaginary parts,

$$\Sigma(\mathbf{p}, \omega) = \Delta(\mathbf{p}, \omega) - i\Gamma(\mathbf{p}, \omega), \quad (7)$$

we find

$$\rho(\omega) = -\frac{1}{\pi} \sum_{\mathbf{p}} \left\{ \frac{\theta(\mu - \omega) \Gamma(\mathbf{p}, \omega)}{[\omega - \mathbf{p}^2/2m + \Delta(\mathbf{p}, \omega)]^2 + \Gamma^2(\mathbf{p}, \omega)} \right\}. \quad (8)$$

It is clear from this expression that the interaction has two effects. It broadens all states so that, for a given  $\omega$ , a range of momenta contribute to  $\rho$ , and produces a level shift of amount  $\Delta$ . Both effects play a role in determining the state density function.

Diagrammatic techniques for evaluating the propagator have been developed by Luttinger and Ward, and extended to the impurity case by Klauder and Langer. We will not discuss the rules for evaluating portions of diagrams involving electron-electron interactions since these are well known. The technique for calculating the contribution of graphs that involve electron-impurity scatterings is somewhat less standard, however, and we will illustrate it by two examples. Following Klauder and Langer we draw the diagrams in such a way that all interactions (dashed lines) associated with a particular impurity are connected to the same point on the diagram. Figure 1 shows two diagrams, involving impurity interactions, that contribute to  $\Sigma(\mathbf{p}, \omega)$ . The first of these illustrates the double scattering of an electron, with momentum  $\mathbf{p}$  and energy  $\omega$ , from the  $I$ th impurity. To calculate the contribution of this graph to  $\Sigma(\mathbf{p}, \omega)$  we insert a factor  $S(\mathbf{p} + \mathbf{q}, \omega)$ , this being the free propagator of the electron, for the particle line between scatterings, and two factors of  $4\pi e^2/\epsilon q^2$  for the Coulomb interaction of the electron with the impurity. The complete contribution of this diagram is obtained by summing over momentum transfers  $\mathbf{q}$  and is

$$\Sigma_2(\mathbf{p}, \omega) = \int \frac{d^3q}{(2\pi)^3} \left[ \left( \frac{4\pi e^2}{\epsilon q^2} \right)^2 S(\mathbf{p} + \mathbf{q}, \omega) \right]. \quad (9)$$

Because the field of the impurity is a static one, there is no energy transfer to an electron in an electron-impurity scattering. Thus, in our example, the electron in the intermediate state has the same energy,  $\omega$ , as it did initially. In this respect electron-impurity interactions differ from, and are simpler than, those of electrons with electrons.

Another feature of the electron-impurity interaction is shown by diagram 1(b), which illustrates a fourth-order process in which an electron interacts with a pair of impurities  $I$  and  $J$ . Because of the ensemble average theorem of Kohn and Luttinger there is momentum conservation ( $\mathbf{q} = \mathbf{q}''$ ) at each impurity vertex. This is a general rule which applies to all impurity vertices. In this sense, as Klauder has emphasized, the positions of the impurities may be treated as quantum mechanical variables.

The foregoing examples illustrate how one is to

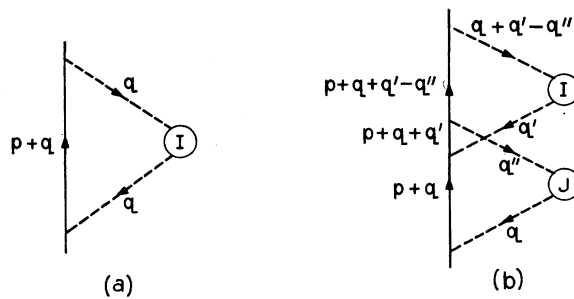


FIG. 1. Graphs involving electron-impurity interactions.

evaluate graphs involving electron-impurity interactions. The special features are: (a) momentum conservation at each impurity vertex and (b) the fact that the impurity interaction, being static, does not change the energy of the scattering electron. With these rules we are now in a position to apply perturbation theory to the calculation of  $\Sigma(\mathbf{p}, \omega)$  [and hence, via Eq. (8), to  $\rho(\omega)$ ]. As a first step in this direction we consider, in the next section, the screening effects of the many-electron system.

### III.

As is well known, the extremely weak falloff of the bare Coulomb potential causes it to have a matrix element that diverges in the limit of zero momentum transfer. Because of this fact it is not possible to express the properties of an electron gas as a power series in  $e^2$ ; attempts to do so inevitably lead to divergent integrals for the coefficients in the expansion. The resolution of this difficulty was given by Mayer<sup>9</sup> (for the classical plasma) and by Gell-Mann and Brueckner, Hubbard<sup>10</sup> and others for the quantum-mechanical situation. They find that, at distances large compared to a Debye length, the interaction of two charges in a plasma is drastically reduced by the polarization of the intervening medium. This effect is one that involves the redistribution of large numbers of electrons. Thus, it is not surprising that to correctly describe it one must sum an infinite subset of the terms in the perturbation series. Another consequence is that the properties of the plasma turn out to be nonanalytic functions of the parameter  $e^2$ .

In terms of the diagrammatic analysis, the correct lowest order screening is obtained by replacing each Coulomb line by a sum over the set of interactions shown in Fig. 2. This series is geometric and is readily summed

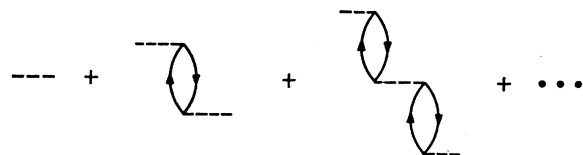


FIG. 2. Graphs that produce lowest-order screening.

<sup>9</sup> J. E. Mayer, J. Chem. Phys. **18**, 1426 (1950).

<sup>10</sup> J. Hubbard, Proc. Roy. Soc. (London) **A240**, 539 (1957).

to give the matrix element

$$\frac{4\pi e^2/\epsilon}{[q^2+(4\pi e^2/\epsilon)R_0(q,\omega)]} \quad (10)$$

of the screened Coulomb interaction. In this expression  $q$  and  $\omega$  are the wave number and frequency carried by the Coulomb line, and  $R_0(q,\omega)$ , the lowest order pair propagator, is the contribution of a single loop in Fig. 2.

As we have seen, in electron-impurity scattering the interaction is a static one. In this case, therefore, the matrix element of Eq. (10) appears with  $\omega$  set equal to zero. Furthermore, the screening term in this formula is only important (to lowest order in  $e^2$ , at least) for small  $q$ . With this approximation the matrix element takes the form of a screened Coulomb potential,

$$4\pi e^2/\epsilon(q^2+\kappa^2). \quad (11)$$

where  $\kappa=[(4\pi e^2/\epsilon)R_0(0,0)]^{1/2}$  is the reciprocal of the Debye length.

In describing electron-electron interactions, which are dynamic processes, it is necessary to use the fully frequency dependent matrix element of Eq. (10). This fact makes the evaluation of higher-order electron correlation effects exceedingly complicated. However, if one is content to work to lowest order in  $r_s$  in evaluating  $\Sigma(\mathbf{p},\omega)$  the difficulties largely disappear. In this approximation the evaluation of the electron-electron self-energy is quite straightforward. We show, in the next section, how it may be calculated and incorporated in a very simple way into the formula for  $\rho(\omega)$ .

#### IV.

In this section we wish to discuss the contributions to  $\Sigma(\mathbf{p},\omega)$  of processes involving electron-electron interactions. The simplest of these arises from the diagram illustrated in Fig. 3(a). Its contribution, however, is exactly canceled by that of diagram 3(b) (involving electron-impurity scattering) since the charges of electron and impurity are opposite. Moreover, it is easy to see that this cancellation persists—essentially because in this particular case (and only here) the electron-electron interaction itself is a static one—when the Coulomb lines of Figs. 3(a) and 3(b) are replaced by the appropriately screened matrix elements of Eq. (10). The physical meaning of this result is clear. It shows that the average potential due to the impurities is exactly canceled by that due to electrons. This is an essentially classical effect and only occurs in diagonal

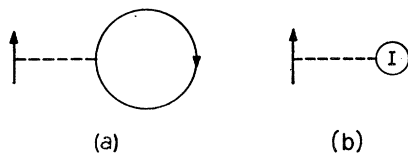


FIG. 3. Diagonal electron interactions.

matrix elements that do not involve any of the true dynamics of the problem. We have dwelt on this point at some length because the band structure of degenerate semiconductors has sometimes been described<sup>1</sup> by a model in which the impurity fields are chosen to be screened Coulomb potentials, and the energy is calculated by taking their *diagonal* matrix elements (this has been called the virtual crystal approximation). It is clear from the above remarks that there is no theoretical justification for this model.

We now proceed to some electron-electron interaction terms that do contribute to  $\Sigma(\mathbf{p},\omega)$ . The simplest of these is the exchange energy, represented by the diagram of Fig. 4(a). Its contribution to  $\Sigma(\mathbf{p},\omega)$  is easily evaluated with the rules given by Luttinger and Ward and turns out to be

$$-\frac{1}{2\pi i} \sum_{\mathbf{q}} \int_{\mu-i\infty}^{\mu+i\infty} e^{\omega'\theta} \frac{4\pi e^2}{\epsilon q^2} \left[ \frac{1}{\omega' - (\mathbf{p}+\mathbf{q})^2/2m} \right] d\omega'. \quad (12)$$

After performing the  $\omega'$  integration we recover the familiar formula<sup>11</sup> for the exchange energy of an electron with momentum  $p$ :

$$-\sum_{\mathbf{q}} \left\{ \frac{4\pi e^2}{\epsilon q^2} \theta \left[ \mu - \frac{(\mathbf{p}+\mathbf{q})^2}{2m} \right] \right\}. \quad (13)$$

This expression increases monotonically from a negative value at  $p=0$  to zero at  $p=\infty$ , and has an infinite derivative at the Fermi surface. The presence of the latter gives rise to a number of difficulties, such as an infinite value of the electronic specific heat. It was early recognized by Wigner,<sup>12</sup> however, that this effect is spurious and that, by including correlation as well as exchange, one would obtain sensible results. The proper way to do this was pointed out by Gell-Mann<sup>13</sup> in his calculation of electronic specific heat. It amounts to replacing the bare, by the screened, Coulomb interaction in Fig. 4(a), thus including diagrams such as those shown in Fig. 4(b). In this approximation the exchange self-energy becomes

$$\Sigma_x(\mathbf{p},\omega) = -\frac{1}{2\pi i} \sum_{\mathbf{q}} \int \frac{d\omega' e^{\omega'\theta}}{[\omega' - (\mathbf{p}+\mathbf{q})^2/2m]} \times \frac{4\pi e^2}{\epsilon[q^2+(4\pi e^2/\epsilon)R_0(q,\omega'-\omega)]} \quad (14)$$

and is, because of the presence of the screening term  $R_0(q,\omega')$ , frequency as well as momentum dependent. Fortunately, however, this effect is not a particularly important one. To order  $r_s$  the screening only affects the energy of electrons in the vicinity of the Fermi

<sup>11</sup> P. A. M. Dirac, Proc. Cambridge Phil. Soc. **26**, 376 (1930); J. Bardeen, Phys. Rev. **49**, 653 (1936).

<sup>12</sup> E. Wigner, Trans. Faraday Soc. **34**, 678 (1938).

<sup>13</sup> M. Gell-Mann, Phys. Rev. **106**, 369 (1957).

surface, and there may be approximated by the zero-frequency and zero-wave-number limit of  $R_0$ . The justification for this procedure is discussed in an Appendix. With its aid we may write Eq. (14) in the form

$$\Sigma_x(\mathbf{p}) = -\sum_{\mathbf{q}} \left\{ \theta \left[ \mu - \frac{(\mathbf{p}+\mathbf{q})^2}{2m} \right] \frac{4\pi e^2}{\epsilon(q^2+\kappa^2)} \right\}, \quad (15)$$

which is just the exchange energy of a free-electron gas as calculated with a screened Coulomb potential. This integral<sup>14</sup> may be evaluated in a straightforward manner and yields the rather cumbersome expression,

$$\Sigma_x(\mathbf{p}) = -\frac{4\pi e^2}{(2\pi)^2 \epsilon} \left\{ \left[ \frac{p_F^2 - p^2 + \kappa^2}{4p} \right] \ln \left[ \frac{(p_F + p)^2 + \kappa^2}{(p_F - p)^2 + \kappa^2} \right] + p_F - \kappa \left[ \tan^{-1} \left( \frac{p + p_F}{\kappa} \right) - \tan^{-1} \left( \frac{p - p_F}{\kappa} \right) \right] \right\}, \quad (16)$$

where  $p_F$  is the Fermi momentum. With this formula one may readily verify, to lowest order in  $r_s$ , that the exchange energies at  $p=0$  and  $p=p_F$  are unchanged by screening. However, the slope at  $p=p_F$  is radically different. Instead of being infinite, its value is given by

$$p_F \frac{\partial \Sigma_x}{\partial p} \Big|_{p=p_F} = \left( \frac{1}{\pi \alpha r_s} \right) \left[ 2 + \ln \left( \frac{\alpha r_s}{\pi} \right) \right] \frac{m e^4}{2 \epsilon^2}, \quad (17)$$

where  $\alpha = (4/9\pi)^{1/2}$ . This is just the Gell-Mann result. Thus the principal effect of the screening is to smooth out the rather abrupt behavior of the unscreened exchange energy in the vicinity of the Fermi surface.

As implied above, Eq. (16) is a rather awkward formula to use in further calculations. To avoid this difficulty we will expand  $\Sigma_x(\mathbf{p})$  about  $p=0$ , writing

$$\Sigma_x(\mathbf{p}) \simeq \Sigma_x(0) + (p^2/2) \Sigma_x''(0), \quad (18)$$

where

$$\Sigma_x(0) = -(4/\alpha \pi r_s) (m e^4 / 2 \epsilon^2) = -\delta, \quad (19)$$

and

$$\Sigma_x''(0) = (1/m) (8\alpha r_s / 3\pi^2). \quad (20)$$

This expression is correct to within about 25% at  $p=p_F$ , and will be used in our subsequent calculations. If we now incorporate the exchange into the free-

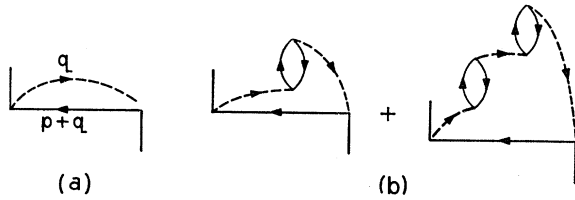


FIG. 4. Exchange self-energy diagrams.

<sup>14</sup> In principle, in evaluating Eq. (15), one should use the perturbed, rather than the zero-order, chemical potential  $\mu$ . The two differ, however, by terms of order  $r_s$ . Thus—since  $\Sigma_x$  itself is of order  $r_s$ —we may use the unperturbed  $\mu$  in evaluating it.

particle propagator we obtain a modified propagator of the form

$$S_x(p, \omega) = \left[ \frac{1}{(\omega + \delta) - (p^2/2m)(1 + 8\alpha r_s/3\pi^2)} \right]. \quad (21)$$

In this approximation inclusion of exchange produces a downward shift of the band by amount  $\delta$ , and changes the mass from  $m$  to  $m^*$ , where

$$\frac{1}{m^*} = \frac{1}{m} \left( 1 + \frac{8\alpha r_s}{\pi^2} \right). \quad (22)$$

The rigid shift of the band structure is similar, though smaller in magnitude, to that predicted by the virtual crystal approximation.

All our subsequent calculations will use the propagator of Eq. (21). Throughout the rest of the problem we may forget electron-electron interaction effects and treat the motion of a *single* electron moving in the screened fields of the impurities, with the propagator  $S_x(p, \omega)$ . With the change of variables  $\omega' = \omega + \delta$  it can be written in the free-particle form

$$S_x(p, \omega') = \frac{1}{[\omega' - p^2/2m^*]}. \quad (23)$$

Thus we see that, to order  $r_s$ , we may take account of electron-electron interactions by screening all impurity interactions, omitting all diagonal matrix elements of the impurity potentials, and modifying the free-particle propagator by a frequency shift and a mass change.

## V.

Having (at least to lowest order in  $r_s$ ) reduced the electron-electron interaction problem to tractable form, we are now in a position to consider electron-impurity scatterings. The simplest such process that contributes to  $\Sigma$  is that illustrated in Fig. 1(a). With the modified propagator, and after summing over impurities, this diagram contributes an amount

$$\Sigma_2(\mathbf{p}, \omega') = n \int \frac{d^3 q}{(2\pi)^3} \left[ \frac{4\pi e^2}{\epsilon(q^2 + \kappa^2)} \right]^2 \left[ \frac{1}{[\omega' - (\mathbf{p} + \mathbf{q})^2/2m^*]} \right] \quad (24)$$

to the self-energy, where  $n$  is the impurity density which we assume to be equal to that of the electrons. This expression may be evaluated by making a change of variables  $\mathbf{p} + \mathbf{q} \rightarrow \mathbf{q}$  and integrating over the directions of  $\mathbf{q}$ . The result is the integral

$$\Sigma_2(\mathbf{p}, \omega') = \frac{8m^* n e^4}{\epsilon^2} \times \int_{-\infty}^{\infty} \frac{q^2 dq}{[(p-q)^2 + \kappa^2][(p+q)^2 + \kappa^2][2m^* \omega' - q^2]}, \quad (25)$$

which may be carried out by contour integration. In performing this calculation  $\omega'$  is assumed to be a complex number; the values of  $\Sigma_2$  to be used in Eq. (5) being obtained by allowing  $\omega'$  to approach the real axis from the lower or upper half-planes. After a fair amount of algebra one finds

$$\Sigma_2(\mathbf{p}, \omega') = \frac{4\pi m^* n e^4}{\kappa \epsilon^2} \left[ \frac{1}{2m^* \omega' - p^2 - \kappa^2 + 2i\kappa(2m\omega')^{\frac{1}{2}}} \right], \quad (26)$$

where  $(2m^*\omega')^{\frac{1}{2}}$  is that branch of the square root that has a positive imaginary part. If we make a cut in the  $\omega'$ -plane from the branch point at  $\omega'=0$  to  $\omega'=\infty$  it then turns out, as Luttinger's<sup>7</sup> analysis indicates should be the case, that  $\Sigma_2(\mathbf{p}, \omega')$  is an analytic function of  $\omega'$  in the cut plane.

Parmenter<sup>1</sup> has previously calculated, using second-order perturbation theory, the energy shift of an electron due to its interaction with screened impurity potentials. To make contact with his work we set  $\omega' \rightarrow \omega$ ,  $m^* \rightarrow m$  in Eq. (26) (thereby omitting shifts due to electron-electron interactions that he did not consider) and, as is proper in straight perturbation theory, work on the energy shell where  $\omega = p^2/2m$ . With these changes we obtain

$$\Sigma_2(\mathbf{p}, p^2/2m) = -\frac{4\pi m n e^4}{\kappa \epsilon^2} \left[ \frac{\kappa^2 + 2ip\kappa}{\kappa^4 + 4p^2\kappa^2} \right]. \quad (27)$$

The real part of this expression is Parmenter's result for the energy shift. In the vicinity of the Fermi surface, however, the imaginary part of  $\Sigma_2$  is considerably larger—by a factor of order  $r_s^{-\frac{1}{2}}$ . Thus, for this energy range, calculation of the density of states requires the inclusion of both level broadening and level shift terms in  $\Sigma$ .

Equation (25) gives the contribution to the self-energy of the simplest diagram that involves electron-impurity scattering. To obtain a density of states function from it we combine Eqs. (5), (6), and (26) and

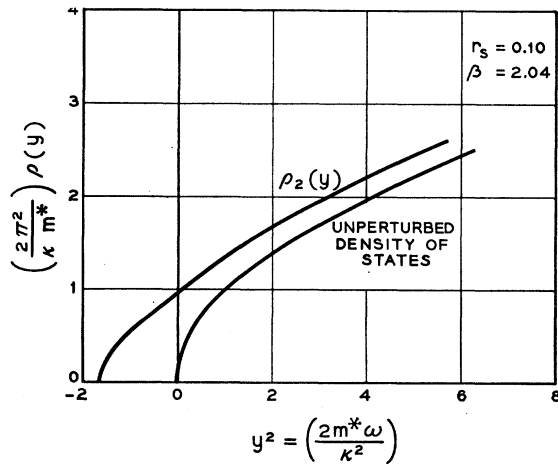


FIG. 5. Density of states vs energy, for  $r_s=0.1$ .

perform the integration over  $p$  indicated in Eq. (5). The integral takes the form

$$\rho_2(\omega) = \frac{\beta m^* \kappa^5 \Gamma^{\frac{1}{2}}}{\pi^3} \times \int_{-\infty}^{\infty} \frac{p^2 dp}{[(\Gamma - p^2)^2 - \kappa^2(\Gamma - p^2) - \beta \kappa^4]^2 + 4\kappa^2 \Gamma (\Gamma - p^2)^2}, \quad (28)$$

where

$$\begin{aligned} \Gamma &= (2m^*\omega')^{\frac{1}{2}}, \\ \beta &= (\pi/12)(\pi/\alpha r_s)^{\frac{1}{2}}. \end{aligned} \quad (29)$$

Equation (28) could, in principle, be evaluated by contour integration. The result, however, is exceedingly complicated and it appears to be easier to calculate the integral numerically for various values of  $\omega'$  and  $r_s$ . Curves obtained in this way for  $r_s=0.1$  and  $0.3$  are illustrated in Figs. 5 and 6. We see that, as compared

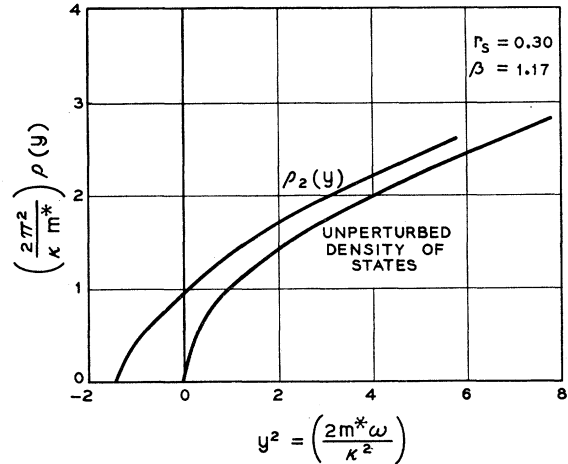


FIG. 6. Density of states vs energy, for  $r_s=0.3$ .

to the unperturbed density of states, the  $\rho_2(\omega)$  curve is shifted downward in energy. This effect is almost exclusively due to the change from  $\omega$  to  $\omega'$  [see Eq. (23)] and thus has its origin in the electron exchange interaction. The corresponding mass change ( $m \rightarrow m^*$ ) is, for the examples illustrated here, quite small. There is also evidence, particularly for the case  $r_s=0.1$ , of some structure near the bottom of the band. This is of the general sort found by Parmenter but should not be taken seriously since, as the discussion of the next section will make clear, the straightforward perturbation series is divergent in this energy range. We do feel, however, that the results presented in Figs. 5 and 6 correctly describe, to order  $r_s$ , the behavior of the density of states near the Fermi surface.

## VI.

In the preceding section we have evaluated  $\rho(\omega)$  taking account of lowest order interactions in calculat-

ing  $\Sigma(\mathbf{p}, \omega)$ . We now wish, by considering higher-order electron-impurity diagrams, to investigate the convergence of our expansion, and suggest ways of improving it, particularly lower down in the band. These considerations will be of a very qualitative nature and will merely suggest the region of convergence of the series; more exact estimates await explicit evaluation of higher-order diagrams.

In going to higher order, two types of diagrams come into consideration; those of the type shown in Fig. 7(a) in which an electron interacts many times with a single impurity atom, and those, such as 7(b), in which an electron interacts with more than one impurity. In the limit  $r_s \ll 1$  one may readily show that diagram 7(a) is, for all momenta  $p$ , small compared to that of Fig. 1(a). This is a general result and we may, therefore, ignore diagrams in which an electron interacts more than twice with a given impurity. Graph 7(b) is more complicated. In it the electron interacts with a pair of impurities and its contribution to  $\Sigma(\mathbf{p}, \omega)$ , in contrast to that of 7(a), is proportional to the square of the impurity density. Since this quantity is large graph 7(b)

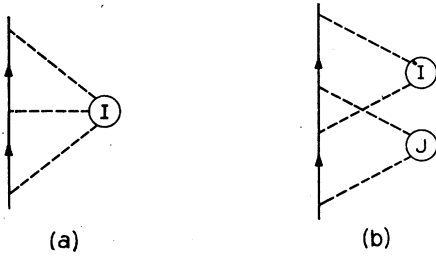


FIG. 7. Higher order electron-impurity interactions.

can, for some values of  $p$ , give a contribution comparable to that obtained from 1(a). To estimate its magnitude we note that, as compared to diagram 1(a), it contains two more Coulomb interactions, two more energy denominators, and an extra integration (over the variable  $\mathbf{q}'$ ). Furthermore, there is an additional factor of impurity density since we here sum over both  $I$  and  $J$ . Considering the order of magnitude, the Coulomb interactions bring in factors  $e^2/\epsilon\kappa^2$ , the energy denominators are about  $p^2/2m - (\mathbf{p} + \mathbf{q})^2/2m \simeq pq/m \simeq p\kappa/m$ , and the extra integration gives—because of the cutoff in the Coulomb matrix element—a factor  $\kappa^3$ . In this very crude way we estimate that the ratio of the contributions of diagrams 7(b) and 1(a) is given by

$$\lambda = O\left[n \left(\frac{e^2}{\epsilon\kappa^2}\right)^2 \frac{\kappa^3 m^2}{(p\kappa)^2}\right] = O\left(r_s^{\frac{1}{2}} \frac{E_F}{E}\right), \quad (30)$$

where  $E_F$  is the Fermi energy, and  $E = p^2/2m$  is, roughly speaking, the energy of the electron. For  $E = E_F$  we have  $\lambda = O(r_s^{\frac{1}{2}})$  and the series should, according to this very primitive estimate, converge. Unfortunately, for smaller values of  $E$ , the convergence soon becomes

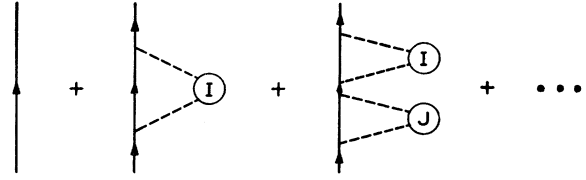


FIG. 8. Modified self-energy diagram.

poorer and for  $E < r_s^{\frac{1}{2}} E_F$  the straightforward perturbation theory appears to diverge.

To obtain a more convergent expansion of the self-energy one may, as the work of Klauder<sup>6</sup> indicates, perform an appropriate partial summation of the perturbation series. The simplest step in this direction consists in replacing every bare electron propagator in a self-energy diagram by a modified propagator that includes the second-order self-energy. In diagrammatic terms this amounts to replacing each internal electron line by the sum of the set of diagrams illustrated in Fig. 8. As is well known, this series may be summed directly; the result is a corrected propagator,

$$S_2(\mathbf{p}, \omega') = \left[ \frac{1}{\omega' - p^2/2m^* - \Sigma_2(\mathbf{p}, \omega')} \right], \quad (31)$$

that includes the second-order self-energy. No detailed calculations using  $S_2(p, \omega')$  to evaluate  $\rho(\omega')$  have as yet been carried out, although it is hoped that they will be in the near future. The behavior of the lowest-order curve for  $\rho(\omega)$  suggests, however, that the change from  $S$  to  $S_2$  will improve the convergence of the series. Figures 5 and 6 indicate that impurity interactions tend to pull the bottom of the band to lower energies. Very crudely, we may say that electrons near the bottom of the band have a lighter-than-normal effective mass. If this is correct, the energy denominators that appear in Eq. (30) will be somewhat larger than we estimated there and the expansion with the propagator  $S_2$  should converge somewhat better than the simple perturbation series. It will be interesting to see whether or not this idea is borne out by detailed calculations.

Assuming that the convergence is improved by replacing  $S$  by  $S_2$ , we may then calculate a better value of  $\Sigma$  by inserting  $S_2$  in Eq. (24). In this way we obtain a corrected self-energy,

$$\bar{\Sigma}_2(\mathbf{p}, \omega') = n \int \frac{d^3q}{(2\pi)^3} \left[ \frac{4\pi e^2}{\epsilon(q^2 + \kappa^2)} \right]^2 \times \left[ \frac{1}{\omega' - (\mathbf{p} + \mathbf{q})^2/2m^* - \Sigma_2(\mathbf{p} + \mathbf{q}, \omega')} \right].$$

Substitution of the result into Eq. (6) should then yield an approximation to  $\rho(\omega)$  that is valid to lower values of  $\omega$  than that plotted in Figs. 5 and 6.

The present problem is one in which one might expect, on quite general grounds, that the use of modified

propagators would lead to considerable improvement in the calculation of  $\rho(\omega)$ . For  $r_s \ll 1$ , many impurities lie within range of one another. Thus, during the scattering of an electron from a particular impurity in the crystal, one would expect to be able to replace the effect of the other impurities by some sort of average field. This is exactly what is done by the propagator modification we have described. It is also clear, however, that the perturbation method will never be useful for calculating  $\rho(\omega)$  at the bottom of the band. Since, when  $r_s \ll 1$ , no single impurity can bind an electron, tightly-bound states can only arise from statistical fluctuations that give clumps of impurities. In this case one must treat, in detail, the interaction of the electron with several impurities. This problem appears to be far too difficult to treat by the perturbation methods we have discussed here.

#### ACKNOWLEDGMENTS

The author would like to express his thanks to R. Brout, E. O. Kane, and J. R. Klauder for a number of stimulating conversations on the topics discussed in this paper, and to J. Schultz for discussion and a critical reading of the manuscript.

#### APPENDIX

We wish here to show that, to order  $r_s$ , the exchange energy may be correctly calculated with a static screened Coulomb potential. To do this, we consider the expression

$$-\left(\frac{1}{2\pi i}\right) \sum_{\mathbf{q}} \int \left(\frac{4\pi e^2}{\epsilon}\right) \frac{d\omega' e^{\omega'0^+}}{[\omega' + \omega - (\mathbf{p} + \mathbf{q})^2/2m]} \times \left\{ \frac{1}{[q^2 + (4\pi e^2/\epsilon)R_0(q, \omega')] } - \frac{1}{[q^2 + (4\pi e^2/\epsilon)R_0(0, 0)]} \right\}, \quad (\text{A1})$$

which represents the difference of the exchange energies, as calculated with and without frequency dependence in the screening factor. The screening is only important, to lowest order in  $r_s$ , for small  $q$ . Thus, we may replace

$R_0$  by its small- $q$  limit, which is easily shown to be

$$R_0(q, \omega') \simeq \frac{4m\hbar_F}{(2\pi)^2} \left\{ 1 - \left(\frac{m\omega'}{2q\hbar_F}\right) \ln \left[ \frac{(m\omega'/q\hbar_F) + 1}{(m\omega'/q\hbar_F) - 1} \right] \right\}. \quad (\text{A2})$$

After the change of variables  $\omega' \rightarrow q\hbar_F x/m$ , expression (A1) takes the form

$$-\left(\frac{1}{2\pi i}\right) \sum_{\mathbf{q}} \int \frac{4\pi e^2 (q\hbar_F)}{\epsilon} \frac{dx e^{x0^+}}{[(q\hbar_F x/m) + \omega - (\mathbf{p} + \mathbf{q})^2/2m]} \times \left\{ \frac{1}{[q^2 + \kappa^2(x)]} - \frac{1}{[q^2 + \kappa^2(0)]} \right\}, \quad (\text{A3})$$

where

$$\kappa^2(x) = \kappa^2 \left[ 1 - \frac{x}{2} \ln \left( \frac{x+1}{x-1} \right) \right]. \quad (\text{A4})$$

We are interested in cases in which  $\omega \simeq p^2/2m$  (to order  $r_s$ ). With this approximation Eq. (A3) may be rewritten in the form

$$-\left(\frac{1}{2\pi i}\right) \int \frac{q^2 dq d\mu}{(2\pi)^2} \left(\frac{4\pi e^2}{\epsilon}\right) \frac{dx e^{x0^+}}{(x - \hbar\mu/\hbar_F)} \times \frac{[\kappa^2(0) - \kappa^2(x)]}{[q^2 + \kappa^2(x)][q^2 + \kappa^2(0)]}, \quad (\text{A5})$$

where  $\mu$  is the cosine of the angle between the vectors  $\mathbf{p}$  and  $\mathbf{q}$ . After carrying out the  $q$  and  $\mu$  integrations, this expression takes the form

$$-\left(\frac{1}{8\pi^2 i}\right) \left(\frac{e^2}{\epsilon}\right) \left(\frac{\hbar_F}{\hbar}\right) \int dx e^{x0^+} \ln \left| \frac{x + \hbar/\hbar_F}{x - \hbar/\hbar_F} \right| [\kappa(0) - \kappa(x)] = -\left(\frac{1}{8\pi^2 i}\right) \left(\frac{\kappa e^2}{\epsilon}\right) \left(\frac{\hbar_F}{\hbar}\right) \int \ln \left| \frac{x + \hbar/\hbar_F}{x - \hbar/\hbar_F} \right| \times \left[ \frac{x}{2} \ln \left( \frac{x+1}{x-1} \right) \right]^{\frac{1}{2}} e^{x0^+} dx. \quad (\text{A6})$$

The coefficient of the dimensionless integral in this formula is of order  $r_s^{\frac{3}{2}}$ , thus confirming our earlier assertion that, to order  $r_s$ , the exchange energy may be correctly calculated with a static potential.